

Quantum-confined Stark shifts of charged exciton complexes in quantum dots

J. J. Finley, M. Sabathil, P. Vogl, and G. Abstreiter

Walter Schottky Institut and Physik Department, Technische Universität München, D85748 Garching, Germany

R. Oulton, A. I. Tartakovskii, D. J. Mowbray, and M. S. Skolnick

Department of Physics and Astronomy, The University of Sheffield, Sheffield S3 7RH, United Kingdom

S. L. Liew, A. G. Cullis, and M. Hopkinson

Department of Electronic and Electrical Engineering, Mappin Street, Sheffield S1 3JD, United Kingdom

(Received 9 July 2004; published 24 November 2004)

We probe the permanent excitonic dipole of neutral and positively charged excitons in individual $\text{In}_{0.5}\text{Ga}_{0.5}\text{As}$ self-assembled quantum dots using Stark effect perturbation spectroscopy. A systematic reduction of the permanent excitonic dipole is found as excess holes are controllably added to individual dots containing a single exciton (X^0). Calculations of the few-body states show that this effect arises from a strong, Coulomb-mediated, spatial redistribution of the few-body wave function upon charging. By investigating correlations between the permanent dipole, polarizability, and the emission energy of X^0 for many dots, we also show that the strength of the In:Ga composition gradient is related to the absolute In content.

DOI: 10.1103/PhysRevB.70.201308

PACS number(s): 78.67.Hc, 71.35.Ji, 71.35.Pq

The fully quantized electronic structure of self-assembled quantum dots (QDs) has recently led to many proposals for their use in next generation optoelectronic devices with true quantum-mechanical functionality. Specific examples include the use of charge and spin excitations in isolated dots as quantum bits^{1,2} and the deterministic generation of single photons.³ Each of these proposals relies fundamentally on the enhanced Coulomb interactions in such fully quantized systems that result in millielectronvolt shifts of the fundamental optical gap as the number, orbital configuration, and total spin of the localized carriers change.⁴ Recently, it has been shown that the carrier occupancy of single dots can be electrically controlled using specially designed field-effect structures.⁵ Fine structure in the emission spectra was identified as arising from charged exciton species from which the relative direct and exchange^{5,6} Coulomb energies for different few-body states have been extracted. While these experiments enable measurement of the relative eigenenergies of different few-body states, they provide little direct information on the form of the few-body wave functions, themselves, and how they are modified as carriers are added to the dot. The nature of the exciton wave function determines key parameters, such as the coupling strength to electromagnetic radiation and phonons and, ultimately, the decoherence rate for excitons. Therefore, a soundly based understanding of the influence of such Coulomb driven modifications of the few-body wave function in QDs is of central importance for their future implementation in quantum devices.

In this paper, we investigate the form of the excitonic charge distribution for different few-body states in individual QDs. Our approach, based on Stark effect perturbation spectroscopy, provides direct access to the excitonic permanent dipole (p_z) and polarizability (β). These quantities are intrinsic properties of the wave function and reflect both the nature of the zero dimensional confinement potential and the role of Coulomb interactions in the few-body state. Our results reveal a systematic reduction of p_z as excess holes are added

controllably to the dot, from neutral ($X^0=1e+1h$) to positively charged excitons ($X^+=1e+2h$ and $X^{++}=1e+3h$). Calculations of the electro-optical response of the few-body wave functions provide good quantitative agreement with experiments, demonstrating that the reduction of the dipole arises from a Coulomb driven redistribution of the exciton wave function in the dot upon charging. Surprisingly, we find that the dominant effect of hole charging is a strong lateral expansion (contraction) of the hole (electron) component of the wave function. This controls the reduction of p_z due to a modification of the electron-hole overlap and, consequently, the balance between e - h attractive and h - h repulsive contributions to the total Coulomb energy.

We begin by describing the samples and the single dot spectroscopy results before presenting the calculations and discussing the form of the few-particle wave functions. The devices investigated consisted of a single layer of low density ($\sim 5 \mu\text{m}^{-2}$) $\text{In}_{0.5}\text{Ga}_{0.5}\text{As}$ self-assembled QDs embedded within the intrinsic region of a p -type GaAs Schottky photodiode.⁷ Such structures allow vertical electric fields up to $F_z \sim -150 \text{ kV/cm}$ to be applied⁸ enabling the study of both Stark effect phenomena and controlled hole charging of the dot from the p -contact.

Photoluminescence (PL) spectra were recorded at $T = 5 \text{ K}$ under weak optical excitation, such that the average QD occupancy was in the single exciton limit.⁹ Typical PL results obtained from two representative dots (dot *A* and dot *B*) are presented in Figs. 1(a) and 1(b), respectively, as a function of axial electric field F_z (V_g). For $|F_z| \geq 90 \text{ kV/cm}$ ($V_g \geq +1.75 \text{ V}$) no PL signal is observed due to field ionization of excitons, while PL arising from the charge neutral exciton (X^0) emerges for lower field.⁷ The peak position of X^0 as a function of V_g is plotted in Fig. 1(c) for both dots (filled squares). As $|F_z|$ reduces, X^0 shifts due to the quantum confined Stark effect, the shift being well described by $E(F) = E_0 - p_z \cdot F_z + \beta \cdot F_z^2$, where p_z and β are the permanent

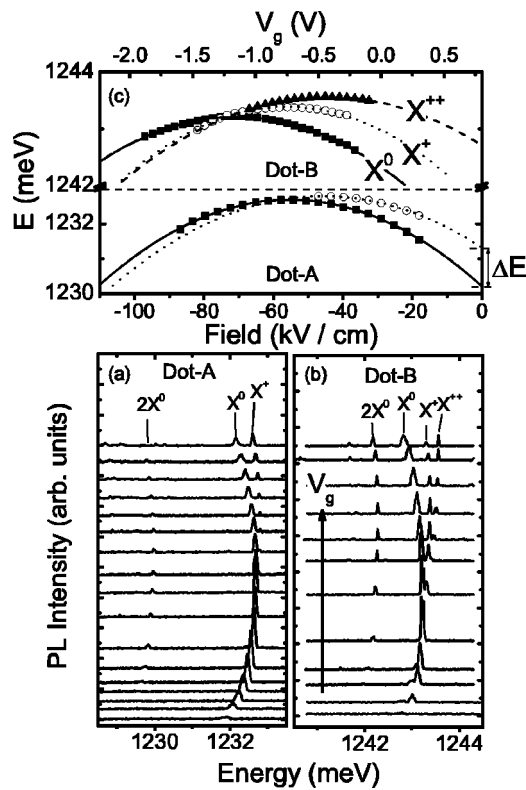


FIG. 1. Single dot PL spectra obtained from (a) dot A and (b) dot B as a function of V_g from +1.9 V (lower trace) to -0.3 V (upper trace). Neutral (X^0) and charged (X^+ , X^{++}) single excitons are observed. (c) Peak positions of the X^0 , X^+ , and X^{++} transitions as a function of V_g/F_z . Parabolic fits to the data are also shown from which p_z and β are extracted.

exciton dipole and polarizability of the state, respectively.¹⁰ The full lines in Fig. 1(a) show the result of such a parabolic fit to the X^0 data from which we extract values of $p_z/e = +0.72 \pm 0.07$ and $+0.89 \pm 0.02$ nm for dots A and B, respectively. For all dots investigated, the positive sign of p_z implies that the electron component of the wave function is located below the hole in the dot at $F_z=0$, signifying In enrichment towards the dot apex.^{10,11}

With decreasing reverse bias, excess holes tunnel into the dot⁵ and one or more additional PL peaks (labeled X^+ and X^{++} in Fig. 1) emerge on the *high*-energy side of X^0 arising from positively charged excitons. The bias range over which these features emerge, together with their splitting from X^0 at $F_z=0$, enable us to identify them as arising from single (X^+) and doubly (X^{++}) charged states. Different charge states are observed simultaneously due to the time integrated nature of the spectra and the comparatively weak tunneling coupling for holes between the dots and the *p* contact.¹² By extrapolating the observed field dependencies for X^0 , X^+ , and X^{++} to $F_z=0$, we measure directly the relative eigenenergies of the different charged exciton states relative to X^0 (ΔE). From a survey of more than 20 dots we measure $\Delta E = +0.7 \pm 0.3$ and $+2 \pm 0.1$ meV for X^+ and X^{++} . These results contrast with the case for negatively charged excitons for which large *red*shifts (up to $\Delta E \sim -5$ meV) are generally observed.⁵ This difference arises due to the smaller spatial extent of the hole wave

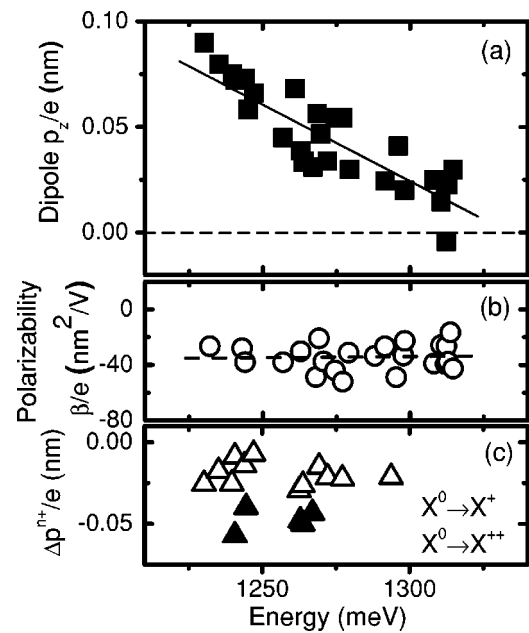


FIG. 2. Summary of (a) p_z and (b) β values measured from many single dots for X_0 plotted as a function of E_0 . (c) Percentage change of exciton dipole upon adding one [$X^0 \rightarrow X^+$ (open symbols)] or two [$X^0 \rightarrow X^{++}$ (filled symbols)] holes.

function and resulting positive-energy contribution.^{5,13}

Also plotted in Fig. 1(c) are the peak positions of the various exciton states together with parabolic fits from which the resulting values of p_z and β are deduced. For X^0 , Fig. 2 shows the values of p_z [Fig. 2(a)] and β [Fig. 2(b)] plotted versus E_0 for more than 20 individual dots. In contrast with Ref. 14 β was found to be uncorrelated with E_0 and p_z , remaining approximately constant over the entire inhomogeneous linewidth with an average value of $\beta/e = -34 \pm 9$ nm²/V. For a particular QD shape and Indium composition profile, β is most sensitive to the dot height (h).¹⁵ This observation enables us to fix h in our calculations presented below. In contrast, p_z and E_0 [Fig. 2(a)] are clearly correlated, the permanent dipole reducing from $\sim +0.8$ to $\sim +0.2$ nm as E_0 increases from ~ 1230 –1310 meV. For a particular QD shape and height, p_z is determined by the In-composition gradient along the QD growth axis, negative dipoles (electron above hole) always being predicted for dots with a homogeneous composition.^{10,15} When taken together, these observations suggest that higher-energy dots possess both a weaker composition gradient (smaller p_z) while their average In content also reduces, tending to increase E_0 . The absence of any β – E_0 correlation demonstrates that the effective height of the dots remains approximately constant, suggesting that the absolute In content and composition profile are not independent variables but that a strong composition gradient also indicates a high In content in the dot and vice versa.

Figure 2(c) shows the absolute change of the exciton dipole [$\Delta p_z^{n+}/e = (p_z^{n+} - p_z^0)/e$] for the charged exciton species relative to X^0 . The most important observation is that Δp_z^{n+} is negative for all dots investigated, implying that the center of gravity of the electron and hole components of the wave

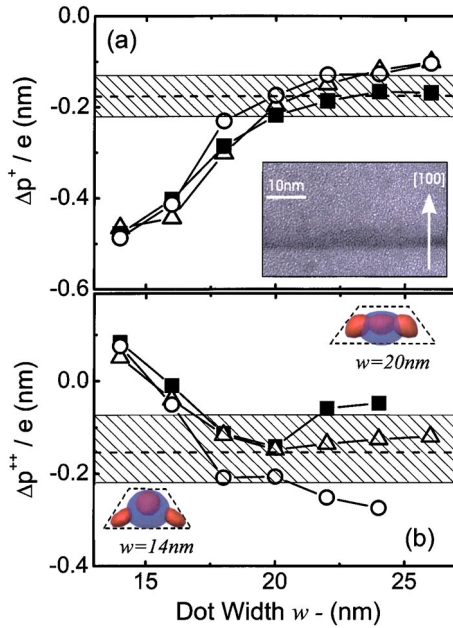


FIG. 3. (Color online) Calculated values of (a) Δp_z^+ and (b) Δp_z^{++} as a function of dot width for linear (squares), inverted pyramidal (circles), and trumpet (triangles) In profiles. The shaded regions show the mean experimental values.

function move closer together as holes are added to the dot. From Fig. 2(c), the mean reduction of p_z upon single hole charging was measured to be $\Delta p_z^+/e = -0.019 \pm 0.003$ nm, whereas for the doubly charged exciton (X^{++}) we measured $\Delta p_z^{++}/e \sim -0.04$ nm relative to X^0 .

In order to explain our experimental observations, we performed calculations of the electronic structure and few-particle states in our dots. We use a one band effective-mass Hamiltonian to calculate the single-particle states including a full treatment of strain and piezoelectric effects.¹⁶ The model QDs are square-based truncated pyramids aligned along the [100] direction with a height of $h=5$ nm needed to reproduce the experimentally observed X^0 polarizability. This parameter depends mostly on the dot height,¹⁵ and further supported by cross-sectional TEM microscopy results [inset, Fig. 3(a)] that revealed dot heights between $h \sim 4-6$ nm. The dot width (w) was chosen as a free parameter and varied in the range $w = 14-26$ nm. Three different composition profiles were investigated with linear,¹⁰ inverted pyramidal¹¹ and trumpetlike¹⁷ In distributions. For fixed w , the lateral confinement potential in the dot becomes progressively stronger when moving from the linear to the inverted pyramidal and trumpetlike profiles.

Few-body interactions were treated by self-consistent solutions of the Kohn–Sham equations accounting for the exchange and correlation Coulomb potential within the local spin-density approximation. For QDs, this approach tends to overestimate the correlation and exchange contributions to the total Coulomb energy by a few meV. This is comparable to the size of the Coulomb charging shifts (ΔE) and it is, therefore, unrealistic to attempt to fit the absolute transition energies of the various charge states at zero field. Instead, our approach is to investigate the response of the few-body

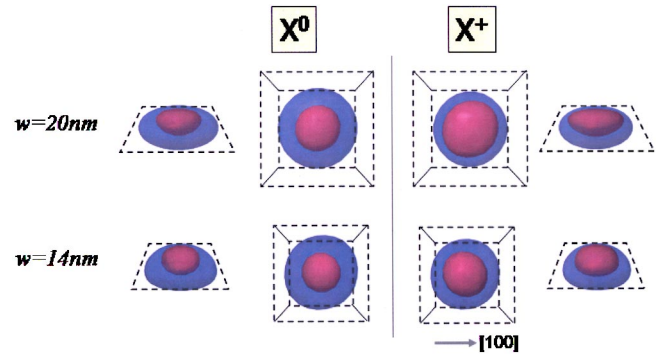


FIG. 4. (Color online) Electron and heavy hole $\sim 50\%$ constant probability isosurfaces for X^0 and X^+ for QDs having a width of $w=14$ and 20 nm. As described in the text, the lateral redistribution of the electron and hole components of the wave function can clearly be seen.

states to static electric fields, i.e., to fit E_0 , p_z , and β for X^0 and then to deduce the change of p_z upon adding one (Δp_z^+) or two (Δp_z^{++}) holes to the dot. The results are plotted in Figs. 3(a) and 3(b), with the shaded regions showing the experimentally deduced values and their associated errors for a dot with a ground-state energy of $E_0=1250$ meV.

We first examine the change of the permanent dipole due to the addition of a single excess hole ($X^0 \rightarrow X^+$) as presented in Fig. 3(a). Similar results were obtained for the three lateral composition profiles, the dot width being the dominant parameter. Our calculations reproduce quite generally the experimentally observed reduction of p_z upon charging over the entire range of w investigated. The magnitude of $\Delta p_z^+/e$ shows two distinct regimes. For $w \geq 20$ nm $\Delta p_z^+/e$ saturates around ~ -0.15 nm, in excellent quantitative agreement with the experimentally observed value of -0.19 ± 0.03 nm [shaded area, Fig. 3(a)]. In contrast, for $w \leq 20$ nm the reduction of the dipole becomes progressively larger, reaching $\Delta p_z^+/e \sim -0.5$ nm for $w \sim 14$ nm, almost $\sim 3 \times$ larger than our experimental finding. Thus, the calculations predict that the QDs investigated here have $w \geq 20$ nm. This result is in good quantitative agreement with the lateral size of our dots deduced from TEM microscopy of ~ 23 nm [inset, Fig. 3(a)] providing further support for the validity of our theoretical approach.

In an effort to understand the physical origin of the w dependence of our $\Delta p_z^+/e$ calculations we examined the form of the few-body wave functions for X^0 and X^+ . Figure 4 shows calculated 50% constant probability isosurfaces of the electron (blue) and hole (red) components of the wave function for two model dots with $w=14$ and 20 nm representing the two size regimes discussed above. For the $w=20$ -nm dot, injecting an additional hole results in a marked (~ 2 nm) expansion of the two-hole wave function in the *plane* of the dot and a commensurate contraction of the one-electron wave function. This redistribution is driven by Coulomb interactions and reflects the tendency of the system to minimize the repulsive $h-h$ interaction whilst maximizing the attractive $e-h$ contribution. The potential for Coulomb limited lateral redistribution of the e and h wave functions upon charging in larger dots explains the origin of the saturation

behavior of $\Delta p_z^+/e$ for $w \geq 20$ nm. The comparatively small reduction of the dipole (~ -0.1 nm) then arises due to enhanced electron-hole attraction in the $2h-1e$ system, which pulls the centers of the $2h$ and $1e$ wave functions together. In contrast, for the $w \sim 14$ -nm dot the lateral redistribution of the wave function is partially suppressed by the stronger lateral quantization and the hole wave function instead expands vertically in the QD upon charging. These effects lead to larger values of $\Delta p^+/e$ as is clearly visible in the cross-sectional images of the wave functions presented in Fig. 4.

The dependence of Δp^{++} on w is calculated to be opposite to that for Δp^+ as discussed above. The X^{++} state is particularly revealing since the four-particle ($3h+1e$) wave function involves the first excited hole p state. As for the case of X^+ discussed above, the calculations for the three composition profiles are similar for $w \leq 20$ nm, diverging more strongly for larger w . One of the most interesting features of the calculated curve is the prediction of an inversion of the sign of the dipole shift for small dots, in strong contrast with the behavior and discussion of X^+ presented above. A qualitative picture of the underlying physics can be obtained by examining the constant energy surfaces of the s - and p -orbital components of the heavy-hole wave function as shown by the insets in Fig. 3(b). For larger dots, the three holes are coplanar and localized toward the top of the dot. This tends to concentrate the Coulomb $e-h$ attraction and reduce the dipole as discussed for X^+ above. In contrast, for narrow dots

the excited hole state shifts toward the base of the dot due to the tapering geometry. This partially balances the net $e-h$ attraction and results in positive values of Δp_z^{++} for $w \leq 16$ nm and negative values when the three holes are coplanar, such as is the case for larger dots. Again, the best agreement with experiment is obtained for $w \geq 20$ nm in excellent accordance with the findings for Δp_z^+ discussed above and in our TEM-microscopy results. The inverted pyramidal and trumpetlike In profiles provide the best quantitative agreement; the linear profile consistently underestimating the magnitude of Δp_z^{++} . This provides direct spectroscopic evidence for recent high-resolution structural microscopy results^{11,18} that have indicated both vertical and lateral variations of the In content throughout the body of the dots grown by the Stranski–Krastanow method.

In summary, from analysis of experimental data obtained by Stark effect perturbation spectroscopy with the help of a detailed theoretical model we were able to predict the form of the charge distribution for different few-particle states in individual InGaAs quantum dots. Our measurements reveal a very pronounced redistribution of the electron and hole components of the wave function as additional holes are sequentially added to the system. The magnitude of these effects, which are driven by Coulomb interactions, were found to be in good quantitative agreement with calculations of the few-body wave functions for several distinct few-body states (X^0 , X^+ , and X^{++}).

-
- ¹A. Barenco, D. Deutsch, A. Ekert, and R. Jozsa, *Phys. Rev. Lett.* **74**, 4083 (1995).
- ²A. Imamoglu, D. D. Awschalom, G. Burkard, D. P. DiVincenzo, D. Loss, M. Sherwin, and A. Small, *Phys. Rev. Lett.* **83**, 4204 (1999).
- ³N. Gisin, G. Ribordy, W. Tittel, and H. Zbinden, *Rev. Mod. Phys.* **74**, 145 (2002), and references therein.
- ⁴P. Hawrylak, *Phys. Rev. B* **60**, 5597 (1999); G. A. Narvaez and P. Hawrylak, *ibid.* **61**, 13753 (2000).
- ⁵R. J. Warburton, C. Schäfflein, D. Haft, F. Bickel, A. Lorke, K. Karrai, J. M. Garcia, W. Schoenfeld, and P. M. Petroff, *Nature (London)* **405**, 926 (2000).
- ⁶B. Urbaszek, R. J. Warburton, K. Karrai, B. D. Gerardot, P. M. Petroff, and J. M. Garcia, *Phys. Rev. Lett.* **90**, 247403 (2003).
- ⁷R. Oulton *et al.*, *Phys. Rev. B* **66**, 045313 (2002).
- ⁸The sign convention adopted in this paper is chosen such that positive F_z is along the growth direction, i.e., orientated from base to tip of the QD.
- ⁹J. J. Finley *et al.*, *Phys. Rev. B* **63**, 073307 (2001).
- ¹⁰P. W. Fry *et al.*, *Phys. Rev. Lett.* **84**, 733 (2000).
- ¹¹T. Walther, A. G. Cullis, D. J. Norris, and M. Hopkinson, *Phys. Rev. Lett.* **86**, 2381 (2001); D. M. Bruls, J. W. A. M. Vugs, P. M. Koenraad, H. W. M. Salemink, J. H. Wolter, M. Hopkinson, and M. S. Skolnick, *Appl. Phys. Lett.* **81**, 1708 (2002).
- ¹²M. Baier, F. Findeis, A. Zrenner, M. Bichler, and G. Abstreiter, *Phys. Rev. B* **64**, 195326 (2001).
- ¹³D. V. Regelman, E. Dekel, D. Gershoni, E. Ehrenfreund, A. J. Williamson, J. Shumway, A. Zunger, W. V. Schoenfeld, and P. M. Petroff, *Phys. Rev. B* **64**, 165301 (2001).
- ¹⁴R. J. Warburton, C. Schulhauser, D. Haft, C. Schäfflein, K. Karrai, J. M. Garcia, W. Schoenfeld, and P. M. Petroff, *Phys. Rev. B* **65**, 113303 (2002).
- ¹⁵J. A. Barker and E. P. O'Reilly, *Phys. Rev. B* **61**, 13840 (2000).
- ¹⁶S. Hackenbuchner, M. Sabathil, and P. Vogl, *Physica B* **314**, 145 (2002).
- ¹⁷M. A. Migliorato, A. G. Cullis, M. Fearn, and J. H. Jefferson, *Phys. Rev. B* **65**, 115316 (2002).
- ¹⁸N. Liu, J. Tersoff, O. Baklenov, A. L. Holmes, Jr., and C. K. Shih, *Phys. Rev. Lett.* **84**, 334 (2000).